

# Zinc Oxide Nanoparticles Synthesized by Microwave-Assisted Combustion Method and Their Potential for Ethanol Gas Detection

L. C. Nehru<sup>1,\*</sup>, C. Sanjeeviraja<sup>2</sup>

<sup>1</sup>Department of Medical Physics, School of Physics, Bharathidasan University, Tiruchirappalli, India

<sup>2</sup>Department of Physics, Alagappa Chettiar College of Engineering & Technology, Karaikudi, India

**Abstract** A facile and rapid microwave-assisted combustion method (MWAC) was developed to synthesis nanocrystalline ZnO powder using dissolution of zinc nitrate (as the oxidant) and glycine (as fuel) as the starting materials and water as solvent, then heating the resulting solution in a microwave oven. The study suggested that application of microwave heating to produce the homogeneous porous ZnO was achieved in few minutes. The starting materials of the combustion product and the influence of the different calcination temperature was discussed based on thermogravimetric analysis and X-ray powder diffraction (XRD). The structure and morphology of the as-prepared and annealed combustion products was investigated by means of XRD and SEM. The average particle size of the nanoparticles synthesized at as-prepared, 400, 500 and 600 °C was calculated to be 20, 27, 29 and 40 nm, respectively. Thick-film sensor samples based on the as-synthesized ZnO nanoparticles without specific additives showed response sensitivity of around 18.05 at the optimal detection temperature of 150 °C for 25 ppm C<sub>2</sub>H<sub>5</sub>OH gas and recovery times were quite fast, of the orders of seconds. The detection limit is lower than the limit needed for breath analyser and the fast dynamics are compatible with a real application also if response to possible interfering gases still have to be investigated.

**Keywords** Nanocrystalline, ZnO, Combustion method, Gas sensor

## 1. Introduction

The fabrication of transition metal oxide semiconductors with nano structure has been the target of scientific interests for gas sensors such as CO, H<sub>2</sub>, H<sub>2</sub>S, C<sub>3</sub>H<sub>8</sub>, C<sub>2</sub>H<sub>6</sub>O, CH<sub>3</sub>COCH<sub>3</sub>, NO and NO<sub>2</sub> [1, 2]. However, these sensing materials can react with several gases simultaneously, and their sensing characteristics (e.g., response, recovery, reproducibility, stability, and linearity) have yet to be improved. Among these oxides, the study of zinc oxide (ZnO) nanostructure is paying considerable attention in many areas of chemistry, physics and material science, mainly due to its broad applications in gas leak detection and environmental monitoring. At 200–400 °C, a resistive electron depletion layer is formed near the surface of the n-type oxide semiconductor by the chemisorption of ambient oxygen. In addition, the interaction between negatively charged surface oxygen and target gases induce large changes in electrical conductivity [3, 4]. Because of high surface-to-volume ratio in gas sensing, the fabrication of a well-defined nano powder

has been the main research approach over the past three decades. However, because many types of reducing and oxidizing gases can interact with the sensing material simultaneously, the selective sensing of a specific gas is not easy to accomplish. The main advantages are the simple sensor structure and operating algorithm. However, these sensing materials react with several gases simultaneously. Various approaches have been introduced to achieve selective gas sensing. Due to the several advantages of ZnO in pure and doped nanomaterials, it gained much importance to study using various methods and their ethanol gas sensing properties [5-11].

However, these methods have some disadvantages, such as complex operating procedures and the high price of raw materials. Furthermore, they generally need high-temperature treatment. The gas-sensing properties were related to the synthesis method and preparation condition, so the response and the detection limit could be improved by changing the synthesis method and optimizing the preparation condition. Many authors proved that the sintering of nanoparticles under standard conditions used for micron-sized particles led to a dramatic growth of particles and to a loss of the nanostructure in the sintered sample. Microwave irradiation as a heating method has found a number of applications in chemistry. The utilization of

\* Corresponding author:

lcnehr@gmail.com (L. C. Nehru)

Published online at <http://journal.sapub.org/ijme>

Copyright © 2016 Scientific & Academic Publishing. All Rights Reserved

microwave irradiation in the preparation of nano particles have been reported in recent years. Compared to the conventional methods, the microwave synthesis have the advantages of producing small particle size metal oxides with high purity owing to short reaction time, enhanced reaction selectivity, and energy saving [12].

Recently, microwave-assisted combustion synthesis is being acknowledged as a novel method to produce materials with an efficient, cost-effective, fast, mild, energy-efficient and environmentally friendly route for easy synthesis of nanosize oxide powders. Since microwave heating is an in situ mode of energy conversion and the microwave heating

process is fundamentally different from conventional heating processes. Heat will be generated internally within the material, instead of originating from external sources. However, there are few reports available using microwave-assisted combustion synthesis method will also be useful for discovering new gas sensor materials as well as in establishing material libraries for gas sensing. The aim of the present work is to synthesize and characterize the microwave-assisted combustion synthesis method prepared ZnO nanoparticles using glycine as fuel and to investigate the ethanol sensing properties of as-synthesized and different calcination temperature of ZnO nanoparticles.

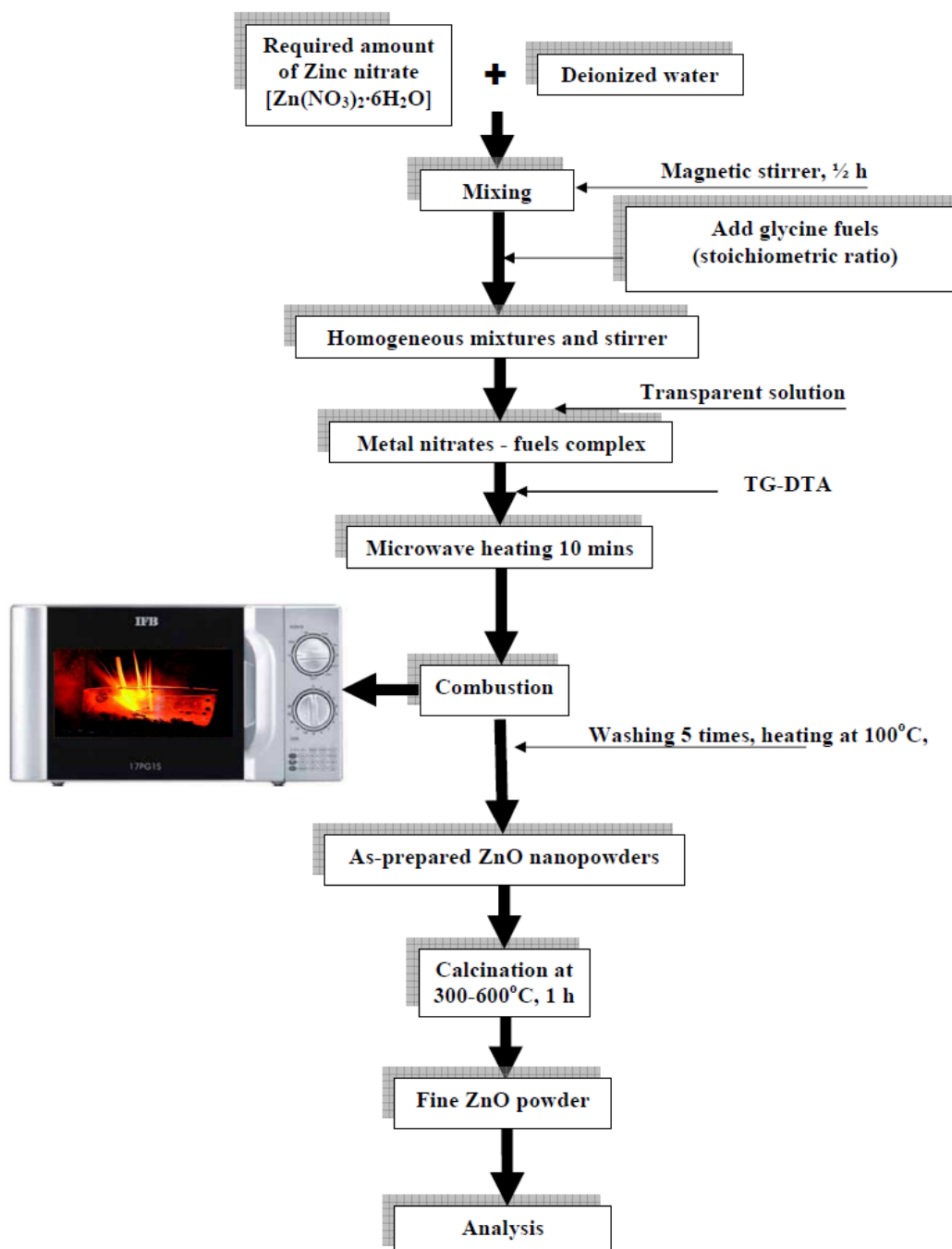


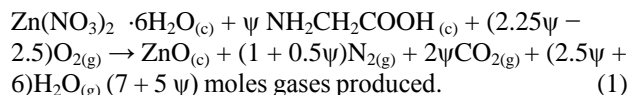
**Figure 1.** Schematic representation of the synthesis process

## 2. Experimental

### 2.1. Preparation of ZnO Nanoparticles

All the reagents used in the experiments were analytically pure and were purchased from MERCK Company, and were used as received without further purification. Nanocrystalline ZnO was synthesized by a microwave-assisted combustion synthesis process using glycine as fuel. A schematic representation of the synthesis process used in the current study is graphically shown in Fig. 1. Stoichiometric amounts of zinc nitrate and glycine were dissolved in deionized water and transferred into a quartz container for mixing well by magnetic stirring for 1/2 h, to make them almost as homogeneous mixture, which further was placed in a domestic microwaveoven (BPL India Limited, Bangalore, India, Model No. IFB, 17PG1S, microwave 700 W, input range 210–230 V-ac 50 Hz, microwave frequency 2.45 GHz). Initially, the solution boils and undergoes dehydration followed by decomposition with the evolution of large amount of gases with white fumes coming out from the exhaust opening provided on the top of the micro oven. After reaching the point of spontaneous combustion in the solution it begins burning and releases lots of heat, vaporizes all the solution instantly and becomes a foamy white solid powder.

Glycine serves as fuel, being oxidized by nitrate. The expected combustion reaction to form ZnO is:



where  $\psi$  is defined as the molar ratio of glycine-to-zinc nitrate corresponds to the situation of an 'equivalent stoichiometric ratio', which implies that the oxygen content of zinc nitrate can be completely reacted to oxidize/consume glycine exactly. As a result, ZnO product and gases of CO<sub>2</sub>, H<sub>2</sub>O and N<sub>2</sub> can be formed directly from the reaction between fuel and oxidizer without the necessity of getting oxygen from outside.

### 2.2. Formation of Thick-Film Sensors

All the sensor samples was fabricated by standard screenprinting thick-film technology. As-prepared ZnO nano powder was mixed and ground with an adhesive in an agate mortar with an aqueous solution of PVA (polyvinyl alcohol) to form a gas-sensing paste. A small amount of zinc powder and glass frit was added in order to improve the film strength and the adhesion to the substrate. The resulting pastes directly coated on alumina substrate which is used to study the ethanol gas sensing properties. The films were then dried at 100 °C for 1 h, to remove PVA in the coated layer. In this screenprinting method, we developed thick films to form a large scale on the substrate and this approach is more reproducible, cost-effective and higher yield process. Electrical contacts were made with copper wire on either side of the thick film sample coated on alumina substract. The central part of the film is exposed to the gas medium.

The sizes of the thick films area are 1 x 1 cm<sup>2</sup> and the active part of the sensor area exposed to the ethanol gas was 0.8 x 0.8 cm<sup>2</sup>. The thickness of the prepared thick films was about 6 to 8  $\mu\text{m}$ .

### 2.3. Characterization

The metal nitrates - fuels complex sample after drying at 80 °C in air for 1/2 h was subjected to thermogravimetric and differential thermogravimetric analysis (TG-DTG) using a Perkin Elmer, Norwalk, CT, USA at a heating rate of 10 °C/min in static air. The synthesized ZnO powders identified the phase formation by powder X-ray diffraction (PXRD) method using a X' Pert PRO PANalytical diffractometer using nickel filtered Cu-K $\alpha$  radiation ( $\lambda=0.15418$  nm) as source and operated at 40 kV and 30 mA. The sample was scanned in the 2 $\theta$  ranging from 10 to 80° in the step scan mode. The observed peak positions were compared with the standard ICDD data and Miller indices were assigned to the Bragg peaks. Morphology of the materials was observed by scanning electron microscope (SEM) (Hitachi S4800). SEM measurements were mounted on aluminum studs using adhesive graphite tape and sputter coated with gold before analysis.

### 2.4. Experimental Set-up and Measurements of Gas-Sensing Properties

The gas-sensing response of the as-prepared ZnO nano powder was characterized by gas-sensing characterization as shown in Fig. 2, where the sensor samples were mounted in a special home made designed gas testing vacuum chamber with controlled temperature and humidity.

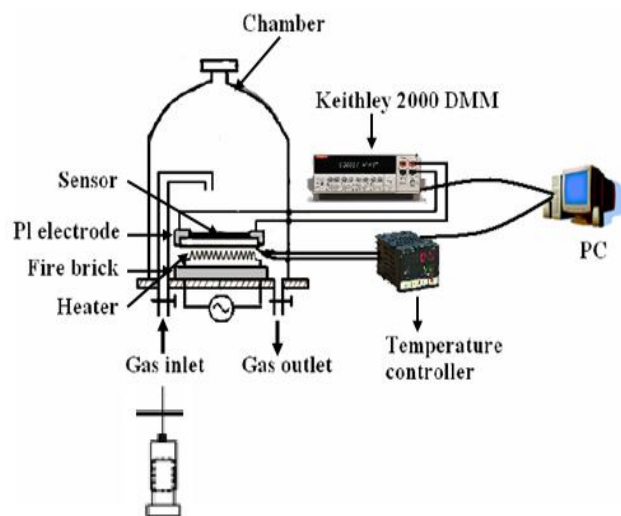


Figure 2. The schematic diagram of the gas sensor measurement setup

The heater was an integrated Ni-Cr heater with a dc voltage controlled by feedback circuitry at operating temperature between room temperature (RT) to 500 °C. The chamber is evacuated to a base pressure of 10<sup>-3</sup> Torr using a rotary vacuum pump. During measurements, the chamber was closed the outlet port and injected ethanol (C<sub>2</sub>H<sub>5</sub>OH) gas (of known concentration) for purging the vacuum chamber

through a gas-injecting fitted with a needle valve using a micro-syringe into the test chamber. The ethanol gas was of 3N purity and was supplied by MERCK. The gas sensing characteristics (in the absence/presence of ethanol gas) was carried out by measuring the electrical resistance change of sensor obtained as follow: first, fresh air was introduced into a chamber and ethanol was injected into the test vacuum chamber. The sensing response characteristics data were recorded using Keithley 2000 Digital multimeter interfaced using Agilent VEE PRO software with a personal computer via a GPIB interface controls. The resistance of the thick film was much larger than the contact resistance; therefore, the two probe method was used instead of the four probe technique. We measured the resistivity of the sample continuously in the presence of ethanol gas (i.e. air + ethanol). The resistance rises quickly at the moment of the introduction of sensor gas and it starts to decrease to the initial level of resistance as soon as the gas stops, i.e the chamber is evacuated. After the chamber was stabilized, we opened the air admittance port so that the air can pump into the chamber. The static method was used for sensing response measurement. The gas concentration was determined by the volume ratio (within the test chamber). Note that the sensor sample was connected in series with a signal resistor ( $R_o$ ). The sensor resistance could be calculated from the output voltage ( $V_o$ ) of the signal resistor which continuously recorded when the sensor was upon gas exposure. The gas response sensitivity ( $S$ ) is defined as the ratio  $(R_a/R_g)^{-1}$ , where  $R_a$  is the sensor resistance in clean air and  $R_g$  is the resistance when sensing responses to the test gas. The prepared gas sensor exhibits desirable sensing characteristics including high sensitivity, fast response and recovery time, good reproducibility, linearity and selectivity.

### 3. Results and Discussion

#### 3.1. Pyrolysis of the Gel

The Figure 3 shows the thermogravimetric and differential thermogravimetric (TG-DTG) curves of the metal nitrates - fuels complex sample after drying at 80 °C in air for 1/2 h.

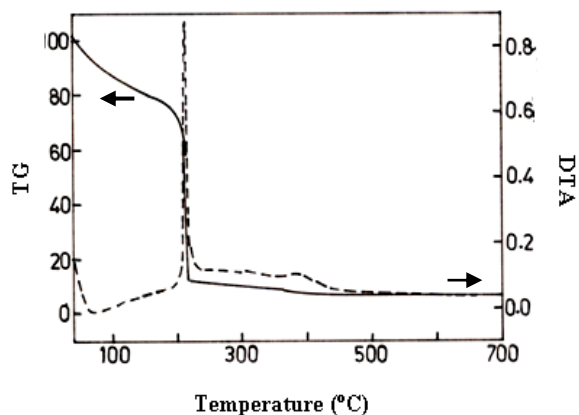


Figure 3. TG/DTA cure of glycine mixed  $Zn(NO_3)_2$

Generally, below 100 °C temperatures are thermally stable and undergo very little physical change. The slight weight loss was probably due to water absorbant either from environment or other volatile impurities. The decomposition occurs suddenly in a single step of strongly exothermic behavior of decomposition at about 210 °C. The maximum weight loss occurs in a very narrow temperature range, which corresponds to the decomposition step. The observed weight loss associated with this exothermic reaction is approximately 56%. By comparing the TG-DTA curves of the precursor and its ingredients, it is suggested that the acceleration of the reaction rate (i.e., the slope of weight loss-temperature curve is very steep) and the lowering of the decomposition temperature arises due to the presence of nitrate ion in the precursor since the  $NO_3^-$  ions provide an in situ oxidizing environment for the oxidation of the organic component.

#### 3.2. Microstructure Analysis

The XRD patterns of powders synthesized at various temperatures of 400–600 °C are shown in Fig. 4. It is indicated with the reflecting planes (1 0 0), (0 0 2), (1 0 1), (1 0 2), (1 1 0), (1 0 3), (2 0 0), (1 1 2) and (2 0 1) in the patterns. All the  $2\theta$  values 31.64, 34.30, 36.13, 47.42, 56.47, 62.74, 66.27, 67.82 and 68.97 ° were well consistent with ASTM (card number 04-008-8198) and no diffraction peaks corresponding to Zn and other impurities were observed, which confirmed the samples as a pure hexagonal wurtzite crystalline ZnO. The value of lattice parameters was calculated by the diffraction angles using the method described elsewhere [13], this results are good agreement with the standard diffraction patterns. It can be seen that the XRD major peaks was broadened. From the particle size measurements, the average particle sizes of ZnO nanoparticles synthesized at as-prepared, 400, 500 and 600 °C was calculated to be 20, 27, 29 and 40 nm, respectively. For the particles synthesized at higher calcination temperatures, XRD peaks became sharper without obvious extension in width. It can be concluded that crystallinity increased with the calcination temperature in the range of 400–600 °C.

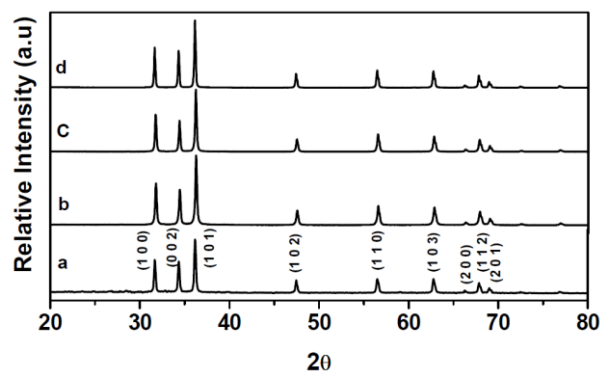
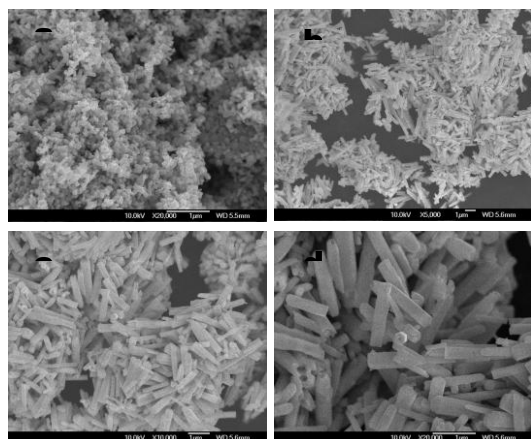


Figure 4. XRD patterns of ZnO synthesized by a microwave-assisted combustion method. (a) as-prepared, (b) calcination temperature at 400 °C, (c) 500 and (d) 600 °C

Figure 5 shows the SEM images of as-prepared ZnO nanoparticles and different calcination temperatures. During calcination process, it can be seen clearly hexagonal shape of the nanorods. Moreover, it is also noticed that the nanorods and ends of nanotubes show clear equilateral hexagon structure as shown in Fig. 5 (d). Only the diameter and lengths of the nanorods and nanotubes changed as the increases of the calcination temperatures. Studying the growth mechanism of nano ZnO, it is possible to suggest that the organic fuel (using glycine) is responsible for the formation of the ZnO nanorod and nanotubes due to the easier complex formation. When glycine are employed, the heat released in combustion is more and as a result the combustion enthalpy is more due to high specific heat capacity, which is responsible for the growth of the sample and complete combustion reaction with small particle size and well-formed nanorods, which might be beneficial for the gas-sensing devices.



**Figure 5.** SEM image of glycine used ZnO nanoparticles with different calcination temperature at (a) as-prepared, (b) 400, (c) 500 and (d) 600 °C for 1 h

### 3.3. Sensing Response Properties

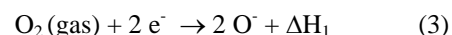
The sensing property of metal oxide-based sensors under ethanol is investigated by allowing ethanol vapor in dry air. The concentration of ethanol vapor in dry air is calculated using the ideal gas equation at room temperature and at atmospheric pressure. According to gas equation  $PV = NkT$  (at STP) where, 'P' is the standard pressure (760 mm of Hg), 'V' is the volume of the chamber (25000 cc) and 'k' is the Boltzmann constant. A known concentration (100 ppm) of ethanol gas was controlled by the injection using a micro-syrings inserted in the vacuum chamber. The injected solvents were completely vaporized on a hot glass plate (about 75 °C). The injection volume ( $V_i$ ) was calculated for the evaluation of gas concentration (c in ppm) by:

$$V_i = \frac{c(ppm) \times V_{chamber} \times MW(g/mol) \times 10^{-3}}{22.45(1/mol) \times D_i(g/ml^{-3})} \quad (2)$$

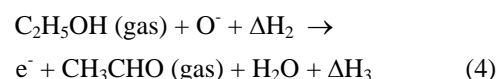
where, the gas constant (22.45 l/mol) means the volume of 1 mol gas at 1 atm, MW denotes the molecular weight of the injected gas and  $D_i$  is the density of the injected sample.

Using these constants, the number of atoms/molecules inside the chamber can be estimated at STP in terms of ppm. Using the gas equation again, the volume of gas to be injected for 1 ppm into the chamber is determined. This volume of the test gas is further used to allow gas concentration of any ppm level.

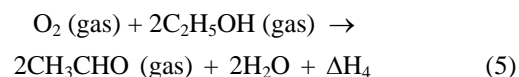
Working temperature have been found to be a crucial parameter for sensor response. So the optimization of work temperature is essential. This temperature sensitive phenomenon are attributed to the over come dynamic energy of activation and reach the maximum S-value that satisfies the sensitizing and detection equation [14] is given below. For sensitizing reaction, reacting gas is adsorbed with contact on the surface of the thick film to form the Schottky contact and the electrical resistance or change in conductivity of these materials.



From the detection reaction, participation of oxygen can be in molecular ( $O_2^-$ ) or in atomic ( $O^-$ ) form to reduce the resistance of the thick film.



On combining these two reactions, the over all reaction on the surface can be given as,



The intermediate product acetaldehyde is also reduced to carbon dioxide and water. The liberation of water saturates the surface and affects the sensitivity. Thus for lower temperature operation, the surface of the sensor does not get completely desorbed which causes smaller change in resistance. As the temperature increases, hydroxyl group are desorbed and decrease in resistance is observed which in turn increases the sensitivity [15, 16]. Also at high temperature, the depletion region created by the chemisorption of oxygen on the surface extends more deeply providing larger scope to more number of gaseous elements to be absorbed thereby giving a better response. Fabricating sensing materials at high temperature may cause coalescence and structural changes to lead sensor instability and response variation. However, low operating temperatures can inhibit structural changes, reduces the power consumption and enables safer detection of combustible gases. Since the sensing mechanism of these devices is based on the chemisorption reaction that take place at the surface of the material, so increasing specific surface area of the sensitive materials leads to more sites for adsorption of surrounding gases.

During the measurements, we injected ethanol gas into the sealed chamber and measured the resistivity of the sample in air and in the presence of ethanol gas. Before exposing to the ethanol gas, the sensor was first stabilized in air for more than 1 h at the working temperature to obtain a stable resistance in air ( $R_a$ ) value. Ethanol was injected into the test rig chamber and sensing response characteristics were

recorded. The gas sensitivity  $S$  ( $S=(R_{\text{air}}-R_{\text{gas}})/R_{\text{gas}}$ ) [17, 18] is plotted against temperature (25 to 300 °C), where  $R_{\text{air}}$  is the sensor resistance in air and  $R_{\text{gas}}$  is the resistance in the presence of reducing gas (ethanol) for each sensor element in air.

The effect of operating temperatures on the sensitivity of the used as-prepared ZnO thick-film sensor samples upon gas exposure at different temperatures (from room temperature to 300 °C) showed response to 25 ppm of  $\text{C}_2\text{H}_5\text{OH}$  were calculated and plotted in Fig. 6. It can be seen that the response sensitivity increased with the temperature, having a maximum of around 46.8 at 150 °C, and then decreased with further rise in temperature. This good response might be associated with the structural and electrical stabilities of as-prepared ZnO nanopowder particles that are beneficial to the development of nanorod microstructure in the thick film, thus providing greater active surface area and gas penetration.

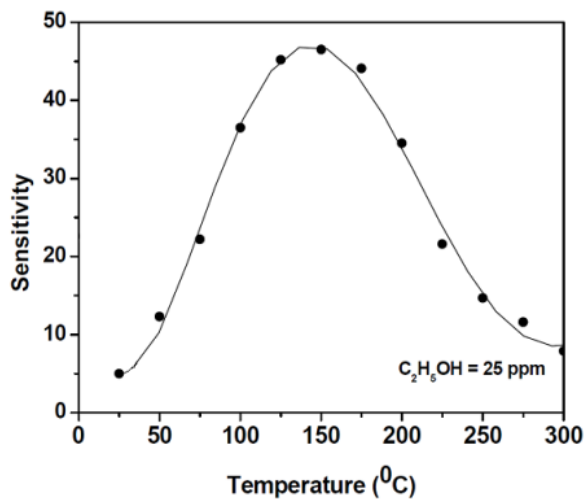


**Figure 6.** Response curve to 25 ppm of  $\text{C}_2\text{H}_5\text{OH}$  gas at different operation temperatures

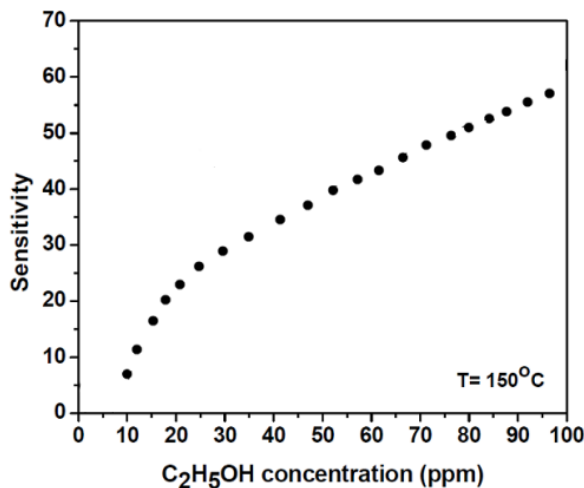


**Figure 7.** Response curve to different concentrations of  $\text{C}_2\text{H}_5\text{OH}$  gas at the optimal temperature ( $T = 150^\circ\text{C}$ )

The as-prepared ZnO thick-film sensor sample exposures

to different ethanol concentration in the range of 1 to 50 ppm at 150 °C temperature (Fig. 7) and some response curves were given in Fig. 8. Both the sensitivity and speed of the response increased monotonically with the concentration of  $\text{C}_2\text{H}_5\text{OH}$  gas, confirming the applicability of pure ZnO nanoparticles in the detection of ppm-level concentrations of  $\text{C}_2\text{H}_5\text{OH}$  gas at relatively low concentration. From Fig. 7 (at 150 °C), the maximum sensitivity of the sensors for  $\text{C}_2\text{H}_5\text{OH}$  gas is observed at 25 ppm.

Fig. 8 shows, it can be seen that the response of the sensor increases and then decreases rapidly of above ethanol concentration. The whole testing-cycle time was set to be 500 s. Semiconductor type gas sensor changes its resistance via the interaction between chemisorbed oxygen with detection gases. Therefore, in the sole viewpoint of the smaller crystalline size with a larger surface area will show higher gas sensitivity. However, the dispersion and configuration of nanorods should also be considered. It is clear from the graph Fig. 6 & 7, a low concentration of 25 ppm ethanol is used for the as-prepared and different calcination temperature ZnO based thick-film sensor sample for sensitivity measurements such as response and recovery properties and low operating temperature (at 150 °C) are very satisfactory. It was also found that the measured device resistivity responded rapidly as we injected ethanol gas into the chamber and pumped them away which indicate that the response speed of the fabricated sensor is also reasonably good. It was found that the as-prepared and various calcination temperatures ZnO based thick-film sensor responds even to 25 ppm  $\text{C}_2\text{H}_5\text{OH}$  gas as shown in Fig. 8. It can be seen from the results at the maximum sensitivity for  $\text{C}_2\text{H}_5\text{OH}$  gas is observed in as-prepared ZnO thick-film sensor sample and the effect of calcination temperature ZnO based thick-film sensor samples were dropped rapidly due to the bigger crystalline sizes. And its response and recovery time is less than 20 to 25 s, respectively. The results show that the sensor has good reversibility and repeatability.

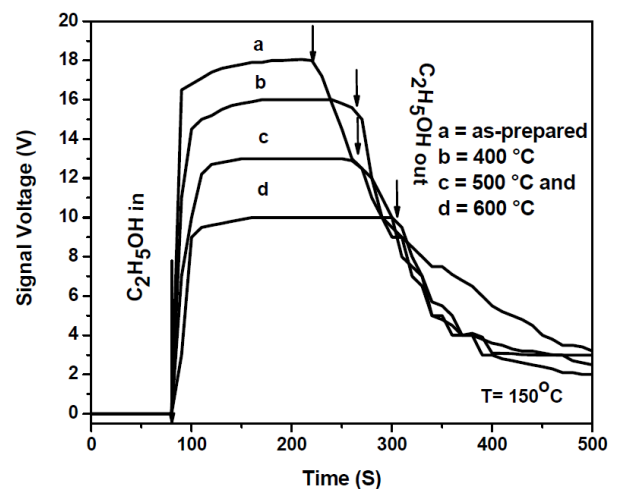


**Figure 8.** The as-prepared and different calcination temperature ZnO based thick-film sensor samples response curves for 25 ppm of  $\text{C}_2\text{H}_5\text{OH}$  gas at optimal temperature ( $T = 150^\circ\text{C}$ )



## 4. Conclusions

The morphology of ZnO nanorods were controlled during the microwave-assisted combustion synthesis method and their C<sub>2</sub>H<sub>5</sub>OH sensing characteristics were investigated. Well dispersed ZnO nanorods could be prepared by adding a small amount of water to the solution containing Zn(NO<sub>3</sub>)<sub>2</sub> · 6H<sub>2</sub>O, and glycine as fuel. The morphological change in the ZnO nanorods was attributed to the various calcination temperatures. At the calcination temperature of 400 to 600 °C, the well-dispersed ZnO nanorods are observed. The present ZnO nanorods are suitable for use in air quality sensor is as a breath analyzer, to detect C<sub>2</sub>H<sub>5</sub>OH in the presence of ethanol vapor in human breath is correlated with the concentration in the blood. Therefore, microwave-assisted combustion synthesis method prepared ZnO have been shown to demonstrate excellent sensing properties.

## REFERENCES

- [1] N. Yamazoe, *Sens. Actuators B* 108 (2005) 2-14.
- [2] M. P. Singh, H. Singh, O. Singh, N. Kohli and R. C. Singh, *Indian J Phys* 86(5) (2012) 357- 361.
- [3] P. S. Cho, K. W. Kim, J H Lee, *J Electroceram* 17 (2006) 975-978.
- [4] K. W. Kim, P. S. Cho, S. J. Kim, J. H. Lee, C. Y. Kang, J. S. Kim, S. J. Yoon, *Sensors and Actuators B* 123 (2007) 318-324.
- [5] N. Yamazoe, G. Sakai, K. Shimanoe, *Catal Surv Asia* 7 (2003) 63-75.
- [6] K. Mirabbaszadeh and M. Mehrabian, *Phys Scr* 85 (2012) 035701-035709.
- [7] B. P. J. D. Costello, R. J. Ewen, N. Guernion, N. M. Ratcliffe, *Sens Actuators B* 87 (2002) 207-210.
- [8] D. F. Paraguay, M. Miki-Yoshida, J. Morales, *Thin Solid Films* 373 (2000) 137 -140.
- [9] X. L. Cheng, H. Zhao, L. H. Huo, S. Gao, J. G. Zhao, *Sens Actuators B* 102 (2004) 248-252.
- [10] I. Stambolova, K. Konstantinov, S. Vassilev, P. Peshev, Ts. Tsacheva, *Materials Chemistry and Physics* 63 (2000) 104-108.
- [11] Xiaoyan Zhou, Qingzhong Xue, Huijuan Chen, Chaozhao Liu, *Physica E: Low-dimensional Systems and Nanostructures* 42 (8) (2010) 2021-2025.
- [12] L. C. Nehru, V. Swaminathan, C. Sanjeeviraja, *Powder Technology* 226 (2012) 29-33.
- [13] A. E. Rakhshani, *Appl Phys A* 81 (2005) 1497-1502.
- [14] H. Windischmann, P. Mark, *J Electrochem Soc* 126 (1979) 627-630.
- [15] D. Kohl, *Sens Actuators B* 18 (1989) 71-114.
- [16] M. R. Vaezi, S. Khoby Shendy and T. Ebadzadeh, *Indian J Phys* 86 (1) (2012) 9-13.
- [17] M. M. Jamshidi, K. Alshaltami, F. Akkari and J. Wright, *Indian J Phys* 87(6) (2013) 511-515.
- [18] M. Mahdizadeh-Rokhi, *Indian J Phys* 87(6) (2013) 517-522.